Atmos. Chem. Phys. Discuss., 9, 1703–1726, 2009
www.atmos-chem-phys-discuss.net/9/1703/2009/

Atmospheric Chemistry and Physics Discussions

Antarctic stratospheric warming since 1979

Y. Hu[1] **and Q. Fu**[2]

[1]Department of Atmospheric Sciences, Peking University, Beijing, China
[2]Department of Atmospheric Sciences, University of Washington, Seattle, USA

Received: 26 November 2008 – Accepted: 4 December 2008 – Published: 16 January 2009

Correspondence to: Y. Hu (yyhu@pku.edu.cn)

Published by Copernicus Publications on behalf of the European Geosciences Union.

Abstract

In the present study, we show evidence of significant stratospheric warming over large portions of the Antarctic polar region in winter and spring seasons, with a maximum warming of 7–8°C in September and October, using satellite Microwave Sounding Unit observations for 1979–2006. It is found that this warming is associated with increasing wave activity from the troposphere into the stratosphere, suggesting that the warming is caused by enhanced wave-driven dynamical heating. We show that the Antarctic stratospheric warming has close correlations with sea surface temperature (SST) increases, and that general circulation model simulations forced with observed time-varying SSTs reproduce similar warming trend patterns in the Antarctic stratosphere. These findings suggest that the Antarctic stratospheric warming is likely induced by SST warming. As SST warming continues as a consequence of greenhouse gas increases due to anthropogenic activity, Antarctic stratospheric warming would also continue, which has important implications to the recovery of the Antarctic ozone hole.

1 Introduction

In the last quarter of the 20th century, one of the most dramatic changes in the stratosphere is severe ozone depletion in the Antarctic spring, i.e. the so-called Antarctic ozone hole. Associated with the severe ozone depletion, the Antarctic stratosphere has displayed strong cooling trends in spring and summer between the late 1970s and the late 1990s (Solomon, 1999; Randel and Wu, 1999; Thompson and Solomon, 2002). It was generally thought that the strong cooling in the Antarctic stratosphere is mainly due to the radiative effect of severe ozone depletion (Ramaswamy et al., 1996; Ramaswamy et al., 2001). In addition, increasing greenhouse gases might also contribute to the observed cooling trends in the Antarctic stratosphere (Shindell and Schmidt, 2004) due to their radiatively cooling effect. The Antarctic stratospheric cooling trends may have important influences on the troposphere and surface climate through altering atmospheric circulations and waves. Indeed, Thompson and Solomon (2002) have linked the Antarctic stratospheric cooling to surface warming over the Antarctic Peninsula.

In contrast to the greatly emphasized Antarctic stratospheric cooling in austral spring and summer and its possible influences on tropospheric climate, here we report stratospheric warming over a large portion of the Southern Hemisphere (SH) high latitudes in austral winter and spring. This regional warming in September and October is especially strong, with maximum warming of 7–8°C since the late 1970s. It is well known that polar stratospheric temperatures are determined by the radiative effects of ozone and greenhouse gases and wave-driven dynamical heating (Andrews, et al., 1987). Because both ozone depletion and increasing greenhouse gases cause cooling in the stratosphere, it is likely that the Antarctic stratospheric warming is due to increasing wave activity. In fact, both the Antarctic polar vortex and planetary wave activity in the SH stratosphere displayed very unusual dynamical behaviour in recent years. That is, the Antarctic stratospheric polar vortex appears to be more frequently and largely disturbed by planetary waves. For example, the unique sudden warming event occurred in the Antarctic in 2002; the vortex was very weak in 2004 due to strong wave activity; and the vortex broke down quite early in 2000 though the ozone hole of that year was anomalously large.

Our main goal in the present study is twofold. First, we document strong Antarctic stratospheric warming trends using both satellite data and reanalysis, and examine whether the warming is caused by increasing wave activity in SH stratosphere. Second, we explore whether the stratospheric warming is related to global greenhouse warming by carrying out general circulation model (GCM) simulations. Satellite and reanalysis datasets and the GCM used in this study are described in Sect. 2. In Sect. 3, we present linear trends in stratospheric temperatures derived from satellite and reanalysis data. We also examine the relationship between Antarctic stratospheric warming and Eliassen-Palm (EP) fluxes. In Sect. 4, we explore the impact of sea surface temperatures (SSTs) on the SH stratospheric warming with GCM simulations. Discussion and conclusions are presented in Sect. 5.

2 Data and model

To detect the Antarctic stratospheric temperature changes in the past few decades, we carry out linear trend analyses using two temperature datasets. The first dataset is 28-year (1979–2006) monthly temperature anomalies from satellite-borne Microwave Sounding Unit (MSU) channel 4 (T_4) observations (Mears et al., 2003; Johanson and Fu, 2006, 2007). MSU T_4 measures microwave radiation emitted from the stratospheric layer between about 20 and 120 hPa, with a peak near 60 hPa (Mears et al., 2003). The second one is 28-year (1979–2006) monthly temperatures from the National Center for Environmental Prediction/National Center for Atmospheric Research (NCEP/NCAR) reanalysis (Kalnay et al., 1996). To calculate Eliassen-Palm (EP) fluxes, we also use daily wind velocity and temperature data from NCEP/NCAR reanalysis. Student t-test is used to test the statistical significance of trends. We use the 90% confidence level (approximately corresponding to the t-test value of 1.7) as the standard for a trend to be statistically significant.

The model used here is the GCM developed at the Goddard Institute for Space Studies (GISS-modelE, Schmidt et al., 2006). The model has horizontal resolution of 4 by 5 degrees in latitude and longitude. It has 23 vertical layers from the surface to 0.02 hPa (about 80 km high) with gravity-wave parameterizations for stratosphere. Five ensemble simulations using different initial conditions were performed over 1950–2002, forced with observed time-varying sea surface temperatures (SST) (Rayner et al., 2003). To isolate the impact of SST warming on the SH stratosphere, ozone and greenhouse gas concentrations are fixed at the 1950 level.

3 Trends in stratospheric temperatures and wave activity

Figure 1 shows the 28-year MSU T_4 trends for SH high latitudes in austral winter and spring months. Warming trends occur in all these months. In June, July, and August, the warming trends are weak and statistically less significant. In September and October, the warming trends are strong and statistically significant, with maximum warming of 7–8°C over the 28 years. In November, cooling trends are dominant, while warming trends are relatively week and less significant. The warming trends are not right over the polar cap, but centered at about 65° S. The temperature trends show a wavenumber-1 like spatially pattern (a secondary wavenumber-2 pattern can also be identified in September), with eastward shifting. The warming area in September matches the climatological location of high temperatures in the SH stratosphere in austral winter and spring. The spatial pattern in October resembles minor sudden warmings in the Arctic stratosphere. It suggests a tendency of the polar vortex shifting off the polar cap. The cooling trends, especially those in October and November, are due to Antarctic ozone depletion, as pointed out in many previous studies (Ramaswamy et al., 1996; Randel and Wu, 1999; Solomon, 1999 among others). It is noticed that the stratospheric sudden warming in 2002 has an important contribution to the warming trends in September and October. However, the maximum warming trends are still up to 5–6°C even if the 2002 warming is excluded, and the spatial trend pattern remains the same (see Fig. 2). In addition, the temperature trend patterns shown in Fig. 1 are remarkably robust and have little dependence on the ending year used in the trend analysis.

For comparison, temperature trends at 70 hPa in SH are also calculated from NCEP/NCAR reanalysis. These trends match satellite-inferred MSU T_4 trends exceptionally well in both spatial pattern and magnitudes in all winter and spring months. To focus on strong warming trends, we only show the results for September and October in Fig. 3a and b, respectively. Again, the 2002 sudden warming does not affect the results (see Fig. 4). Warming trends are found at all stratospheric layers in the reanalysis data. Figure 5 shows 28-year temperature trends in September at 100, 50, 30, and 20 hPa pressure levels. The spatial patterns of warming trends are similar at these levels. Warming magnitude increases with altitudes and reaches the maximum value of about 11°C at 30 hPa. One can also find that the warming trends tilt toward the pole with increasing altitudes.

Warming signals in the Antarctic stratosphere in austral spring were identified in previous studies (Randel and Wu, 1999; Johanson and Fu, 2007). However, conventional zonal or seasonal averages in these studies largely reduced the magnitude of warming trends. For example, due to the strong cooling in November and mismatch of warming locations in September and October, conventional seasonal average over the three months yields a maximum warming of about 2.5°C over the 28 years. Thus, little attention was paid to these warming trends. It is likely that the stratospheric warming has direct linkage with the warming in the Antarctic troposphere in winter and spring, derived from both radiosonde data (Turner et al., 2004) and MSU data (Johanson and Fu, 2007). The tropospheric warming trends in austral spring, which are weaker compared with the stratospheric warming, are also mainly over the eastern side of the Antarctic continent (Johanson and Fu, 2007), consistent with the locations of stratospheric warming trends. At current stage, we are unaware how the warming trends are linked between the stratosphere and troposphere.

The Antarctic stratospheric warming shown above cannot be explained by radiative effects of increasing greenhouse gases and ozone depletion. It is because increasing greenhouse gases in the atmosphere leads to surface and tropospheric warming but stratospheric cooling, and ozone depletion during the past few decades has also contributed to stratospheric cooling, especially in the Antarctic lower stratosphere in spring and summer. It is well known that polar stratospheric temperatures are also crucially determined by planetary-scale waves that are generated in the troposphere (Andrews et al., 1987). As planetary waves propagate upward into the stratosphere, breaking of these waves drives a meridional residual circulation with rising motion in the tropics, poleward flow at mid-latitudes, and downward motion in polar regions (i.e. “Brewer-Dobson circulation”). The polar stratospheric temperature is thus determined by a balance between radiative cooling and dynamic heating from induced vertical motion due to planetary wave dissipation. Therefore, the Antarctic stratospheric warming is likely caused by increased wave activity from the troposphere into the stratosphere. The remarkable agreement of warming trends between MSU T_4 and NCEP/NCAR reanalysis allows us to use the reanalysis to examine decadal changes in wave activity.

To show how changes in wave fluxes cause the strong warming over the SH high-latitude stratosphere in September and October, we plot the 28-year trends in EP flux vectors (arrows) and EP flux divergence (colors) averaged over August–September–October (ASO) in Fig. 5a, using NCEP/NCAR reanalysis. We include EP fluxes in August because wave fluxes in the previous month also contribute dynamical heating in the month considered (Hu and Tung, 2002). The direction of arrows represents the tendency of wave propagation over 1979–2006. Arrows are generally upward between 50° S and 90° S, indicating enhanced wave fluxes from the troposphere into the stratosphere. Arrows from the upper troposphere to the stratosphere between 30° S–50° S are equatorward, suggesting enhanced equatorward wave propagation. EP flux divergence show negative trends in the stratosphere and upper troposphere between about 45° S and 70° S. The negative trends indicate enhanced EP flux convergence in these regions. The significant enhancement of EP flux convergence in the stratosphere suggests an intensified Brewer-Dobson circulation and thus enhanced dynamical heating in the polar stratosphere. On the other hand, EP flux divergence shows strong positive trends in the middle troposphere between about 30° S and 70° S. The positive trends are indicative of increased wave activity generation.

Wave fluxes from the troposphere into the stratosphere can also be measured by total eddy-heat fluxes across the tropopause in middle and high latitudes (Hu and Tung, 2003), which is equivalent to the vertical component of EP fluxes. Figure 5b shows the time series of area-weighted total eddy-heat fluxes at 150 hPa between 40° S and 90° S, averaged over ASO (solid line). It demonstrates a systematic increase of ∼38% over 1979–2006 (solid straight line), with statistical significance above the 99% confidence level. Superimposed on the plot is MSU T_4 temperature for October averaged over the area within which warming trends are larger than 6 K for the 28 years (dashed-line). The correlation between eddy-heat fluxes and temperatures is about 0.5. Note that the correlation coefficient between September temperature and eddy-heat fluxes averaged over August–September is even higher, about 0.8. The close correlation suggests that the Antarctic stratospheric warming is caused by wave-driven dynamical heating.

The much stronger warming in September and October than in other months coincides with the seasonality of the planetary wave activity in the SH stratosphere. Randel (1988) has showed that the amplitudes of wavenumber 1 and 2 in the SH stratosphere reach maxima in September and October. It suggests that enhanced wave-driven dynamical heating is more significant in the period when planetary wave activity is strong. Indeed, our calculations indicate that the increase in wave fluxes from the troposphere into the stratosphere in September and October is much larger than that in June, July, and August. This is because the Antarctic polar night jet is much stronger in winter months than in spring, which tends to prevent upward propagation of planetary waves.

In addition to the contribution from quasi-stationary waves, travelling waves also make an important contribution to the strong warming in September and October. Figure 6 shows the time series of total eddy-heat fluxes for travelling and stationary waves at 150 hPa averaged over ASO, respectively. It shows systematic increase in eddy-heat fluxes of both travelling and quasi-stationary waves since 1979. The net increases of wave fluxes due to travelling and stationary waves are ∼41% and 44%, respectively. Note that travelling-wave fluxes at the tropopause level are actually about one third larger than stationary-wave fluxes. Randel (1988) showed that amplitudes of travelling waves in the SH stratosphere are nearly equal to that of stationary waves. The increasing activity of travelling waves also explains the eastward shifting of warming trend patterns in other months.

Increasing wave fluxes in the middle and high-latitude stratosphere would also cause more ozone to be transported from low to high latitudes. Because the polar night jet tends to blocks air transport into the polar vortex, ozone-rich air is accumulated outside the polar vortex. Thus, enhanced wave flux convergence leads to more ozone accumulation outside the polar vortex, which may also contribute to the observed warming by absorbing more ultraviolet radiation. To examine this, we calculate the trends in total ozone using the satellite Total Ozone Mapping Spectrometer/Solar Backscatter

Ultraviolet observations. A weak ozone increase of ∼5–6 DU for 1979–2006 is found in the warming areas in September and October (figure not shown), which is too small to explain the observed warming radiatively.

4 Relation between stratospheric warming and SST

An important question is what causes the increased planetary wave activity. Early studies suggested that changes in SSTs might lead to changes in SH wave activity, which consequently modulate SH atmospheric circulations (Hurrell and Loon, 1994). Recent studies on the 2002 Antarctic major warming showed that strong wave activity originated from the tropical troposphere (Nishii and Nakamura, 2004). In modelling studies of SST influences on the North Atlantic oscillation (NAO), Hoerling et al. (2001) pointed out that the decadal trends of NAO are originated from tropical SST warming. Studies by Hoerling et al. (2004) and Lau et al. (2005, 2006) further suggested that tropical SST warming in the region of Indian and Western Pacific oceans plays the major role in forcing extratropical tropospheric changes. Therefore, a plausible mechanism responsible for the increasing wave activity and the observed Antarctic stratospheric warming is SST changes.

To verify the relationship between Antarctic stratospheric warming and SST changes, we first examine the correlation of the MSU T_4 in September, averaged over the warming area enclosed by the contour of 6°C per 28 years, with observed global SST (Rayner et al., 2003) for 1979–2006. Figure 7a shows the spatial distribution of correlation coefficients in September. Significant correlations are found mainly over the tropical Indian Ocean and Western Pacific warm pool regions, southern and northern extratropical Pacific, and northern subtropical Atlantic. Correlation between stratospheric temperatures in NCEP/NCAR reanalysis and SST has nearly the same spatial pattern. All these areas show relatively large SST warming trends (Fig. 7b). It suggests that the Antarctic stratospheric warming is largely related to SST warming.

To examine whether the Antarctic stratospheric warming is a response to SST warming, we carry out GCM simulations with prescribed SST and sea ice, using GISS-modelE. Five ensemble members of simulations were performed over 1950–2002, forced with observed monthly time-varying SST (Rayner et al., 2003). Ozone, well-mixed greenhouse gas concentrations, and all other atmospheric compositions are fixed at the 1950 level to isolate the impact of time-varying SST. Figure 9 shows the trends in ensemble-mean monthly temperatures from GCM simulations at 70 hPa for 1979–2002. Warming trends are found over the Antarctic in all winter and spring months, with strong warming in ASO. The lack of stratospheric cooling in GCM simulations (as compared with observations) is because ozone depletion and increasing greenhouse gases are not included in the simulations. The spatial distribution of simulated temperature trends show a wavenumber-1 pattern, with eastward shifting (A secondary wavenumber-2 pattern can also be seen in Fig. 9). The locations of simulated maximum warming trends in August and September match observations very well, while that in October does not due to the lack of eastward shifting. The ensemble-mean maximum warming trend occurs in September and October, which is about 3.5°C over 1979–2002. In June, July, and November, the warming trends are relatively weak, about 1.0°C for the 24 years. It appears that the seasonality of the simulated warming trends is consistent with observations.

Compared with MSU T_4 trends, the simulated warming trends are weaker, which is about half in magnitudes. However, individual simulations show more realistic warming trends. For example, the maximum warming is as large as about 6°C over the 24 years. It is found that the reduction of the warming in ensemble mean is mainly because of the location mismatch of maximum warming trends between individual simulations. The weaker simulated warming than observations in September and October is probably also due to the cold Pole bias in the modelled polar stratosphere, which is a common problem in most GCMs. As the simulated polar stratosphere is colder, the polar night jet is stronger. It causes less wave fluxes into the stratosphere and thus weaker stratospheric responses to SST warming in the GCM. Indeed, our simulations show a much weaker increase in wave fluxes across the tropopause, only about 10% in the 24 years. Nonetheless, the GCM simulation results do suggest that the Antarctic stratospheric warming is closely related to SST warming.

5 Discussion and conclusions

We have shown that the Antarctic stratosphere has been warming in winter and spring months since 1979. The warming trends are particularly strong in September and October. Results from MSU T_4 data show that the maximum warming in the two months is as large as 7–8°C over the 28 years. In NCEP/NCAR reanalysis, the maximum warming is about 11°C at 30 and 20 hPa. The spatial distributions of temperature trends show a wavenumber-1 like pattern, shifting eastward. In September and October, warming trends are located over the eastern side of the Antarctic continent.

The Antarctic stratospheric warming is associated with increasing wave fluxes in the SH stratosphere. Our calculations show significant increased EP fluxes and enhanced EP flux convergence in the midlatitude stratosphere. The enhancement of EP flux convergence leads to intensified residual meridional circulation and thus stronger downward motion in SH high latitudes, which causes enhanced adiabatic heating. These suggest that the warming is due to enhanced wave-driven dynamical heating. Increasing wave fluxes are not only from quasi-stationary waves but also from travelling waves.

The close correlation between stratospheric temperatures in the warming region and SST suggests that the stratospheric warming is due to SST warming. GCM simulations with observed time-varying SST can reasonably reproduce the seasonality and spatial patterns of observed warming trends. The shortcoming of the simulations is that the magnitude of ensemble-mean warming trends are about half of observations. Our simulation results are consistent with that in previous modelling studies which show an enhanced Brewer-Dobson circulation with either prescribed SST or increasing greenhouse gases (Eichelberger and Hartmann, 2005; Butchart et al., 2006). The enhancement of the Brewer-Dobson circulation in these simulations also suggests stratospheric warming in high latitudes through enhanced dynamic heating. Because SST warming is due to increasing greenhouse gases (Knutson and Manabe, 1998; Solomon et al., 2007), the Antarctic stratospheric warming is an integral part of global greenhouse warming.

Previous studies suggested that tropical SST warming, especially SST warming over tropical Indian and western Pacific oceans, plays a major role in forcing changes of atmospheric waves and circulations in the extratropics through remote atmospheric connections (Hoerling et al., 2001, 2004; Lau et al., 2005, 2006). These works mainly focused on extratropical responses on tropical SST warming in the troposphere. In future works, we will examine whether the tropical SST forcing on stratospheric temperatures is in the similar way. We will also carry out detailed analyses on how SST warming causes the increase in wave activity in the extratropical stratosphere, especially planetary wave activity that drives enhanced dynamical heating in stratospheric polar regions. In addition to SST warming, increasing greenhouse gases also causes tropospheric warming and stratospheric cooling. The changes in atmospheric thermal structures would also cause changes in wave activity and atmospheric circulations. Coupled atmospheric-oceanic GCM simulations with increasing greenhouse gases seem to be necessary for future comprehensive studies.

The observed strong Antarctic stratospheric warming in September and October may have important implications for ozone-hole recovery because the Antarctic ozone hole mainly occurs in those two months. It is well understood that extremely low temperatures in Antarctic winter and spring are one of the critical conditions for severe ozone depletion and the formation of the Antarctic ozone hole (Solomon, 1999). Low polar temperatures lead to the formation of polar stratospheric clouds (PSC), on which heterogeneous chemical reactions involving man-made chlorine take place and result in rapid ozone depletion. The cold conditions also cause the strong Antarctic vortex that provides an isolated environment for polar ozone depletion (McIntyre, 1989). As SST warming continues as a consequence of increasing greenhouse gases, Antarctic stratospheric warming will also continue. The warming would cause reduction of the

Title Page
Abstract | Introduction
Conclusions | References
Tables | Figures
◀▏ | ▶▏
◀ | ▶
Back | Close
Full Screen / Esc
Printer-friendly Version
Interactive Discussion

severity and duration of the Antarctic ozone hole by reducing PSCs, which slows down heterogeneous chemical reaction rates. Moreover, the associated increasing wave activity in the SH stratosphere would also cause the Antarctic polar vortex weakened and more ozone transported to the polar region from low latitudes. These will all benefit the recovery of the Antarctic ozone hole, in addition to the decline of ozone depleting substances (Weatherhead and Andersen, 2006; WMO, 2007).

Acknowledgements. Y. Hu is supported by grants from the NSF of China (40575031 and 40533016), the Ministry of Education of China (106002), and the National Basic Research Program of China (2007CB411801). Q. Fu is supported by NOAA and NASA. GCM simulations were done when Y. Hu worked at the Goddard Institute for Space Studies of NASA and Columbia University. We thank D. L. Hartmann, L. Jaegle, C. B. Leovy, and J. M. Wallace for critical discussions and reading of the manuscript.

References

Andrews, D. G., Holton, J. R., and Leovy, C. B.: Middle Atmosphere Dynamics. Academic Press, New York, 489 pp., 1987.

Butchart, N., Scaife, A. A., Bourqui, M., et al.: Simulations of anthropogenic change in the strength of the Brewer-Dobson circulation, Clim. Dynam., 27, 727–741, 2006.

Eichelberger, S. J. and Hartmann, D. L.: Changes in the strength of the Brewer-Dobson circulation in a simple AGCM, Geophys. Res. Lett., 32, L15807, doi:10.1029/2005GL022924, 2005.

Hoerling, M. P., Hurrell, J. W., and Xu, T.: Tropical origins for recent North Atlantic climate change, Science, 292, 90–92, 2001.

Hoerling, M. P., Hurrell, J. W., Xu, T., Bates, G. T., and Phillips, A. S.: Twentieth century North Atlantic climate change. Part II: Understanding the effect of Indian Ocean warming, Clim. Dynam., 23, 391–405, 2004.

Hu, Y. and Tung, K.: Interannual and decadal variations of planetary wave activity, stratospheric cooling, and Northern Hemisphere annular mode, J. Climate, 15, 1659–1673, 2002.

Hu, Y. and Tung, K.: Possible ozone-induced long-term changes in planetary wave activity in late winter, J. Climate, 16, 3027–3038, 2003.

Hurrell, J. W. and Loon, H.: A modulation of the atmospheric annual cycle in the Southern Hemisphere, Tellus A, 46, 325–338, 1994.

IPCC: Climate Change 2007: The Physical Science Basis, Contribution of Working Group I to the Fourth Assessment Report of the Intergovernmental Panel on Climate Changes, edited by: Solomon, S., Qin, D., Manning, M., et al., Cambridge University Press, Cambridge, UK, 996 pp, 2007.

Johanson, C. M. and Fu, Q.: Robustness of tropospheric temperature trends from MSU channels 2 and 4, J. Clim., 19, 4234–4242, 2006.

Johanson, C. M. and Fu, Q.: Antarctic atmospheric temperature trend patterns from satellite observations, Geophys. Res. Lett., 34, L12703, doi:10.1029/2006GL029108, 2007.

Kalnay, E., Kanamitsu, M., Kistler, R., et al.: The NCEP/NCAR 40-year reanalysis project, B. Am. Meteorol. Soc., 77, 437–471, 1996.

Knutson, T. R. and Manabe, S.: Model assessment of decadal variability and trends in the tropical Pacific ocean, J. Climate, 11, 2273–2296, 1998.

Lau, N.-C., Leetmaa, A., and Nath, M. J.: Influences of ENSO-induced Indo-Western Pacific SST anomalies on extratropical atmospheric variability during the boreal summer, J. Climate, 18, 2292–2942, 2005.

Lau, N.-C., Leetmaa, A., and Nath, M. J.: Attribution of atmospheric variations in the 1997-2003 period to SST anomalies in the Pacific and Indian Ocean basins, J. Climate, 19, 3607–3628, 2006.

Mears, C. A., Schabel, M. C., and Wentz, F. J.: A reanalysis of the MSU channel 2 tropospheric temperature record, J. Climate, 16, 3650–3664, 2003.

Nishii, K. and Nakamura, H.: Tropospheric influence on the diminished Antarctic ozone hole in September 2002, Geophys. Res. Lett., 31, L16103, doi:10.1029/2004GL019532, 2004.

Ramaswamy, V., Schwarzkopf, M. D., and Randel, W. J.: Fingerprint of ozone depletion in the spatial and temporal pattern of recent lower stratospheric cooling, Nature, 382, 616–618, 1996.

Ramaswamy, V., Chanin, M.-L., Angell, J., et al.: Stratospheric temperature trends: Observations and model simulations, Rev. Geophys., 39, 71–122, 2001.

Randel, W. J. and Wu, F.: Cooling of the Arctic and Antarctic polar stratosphere due to ozone depletion, J. Climate, 12, 1467–1479, 1999.

Randel, W.: The seasonal evolution of planetary waves in the Southern Hemisphere stratosphere and troposphere, Q. J. Roy. Meteor. Soc., 114, 1385–1409, 1988.

Rayner, N. A., Parker, D. E., Horton, E. B., et al.: Global analyses of sea surface temperature, sea ice, and night marine air temperature since the late nineteenth century, J. Geophys. Res., 108, 4407, doi:10.1029/2002JD002670, 2003.

Schmidt, G. A., Ruedy, R., Hansen, J. E., et al.: Present day atmospheric simulations using satellite and re-analysis data, J. Climate, 19, 153, 2006.

Shindell, D. T. and Schmidt, G. A.: Southern Hemisphere climate response to ozone changes and greenhouse gas increases, Geophys. Res. Lett., 31, L18209, doi:10.1029/2004GL020724, 2004.

Solomon, S.: Stratospheric ozone depletion: a review of concepts and history, Rev. Geophys., 37, 275–316, 1999.

Thompson, D. W. J. and Solomon, S.: Interpretation of recent Southern Hemisphere climate change, Science, 296, 895–899, 2002.

Turner, J., Lachlan-Cope, T. A., Colwell, S. R., Marshall, G. J., and Connolley, W. M.: Significant warming of the Antarctic winter troposphere, Science, 311, 1914–1917, 2006.

Weatherhead, E. C. and Andersen, S. B.: The search for signs of recovery of the ozone layer, Nature, 441, 39-45, 2006.

WMO (World Meteorological Organization): Scientific Assessment of Ozone Depletion: 2006, Global Ozone Research and Monitoring Project, Geneva, Switzerland, Report No. 50, 572 pp., 2007.

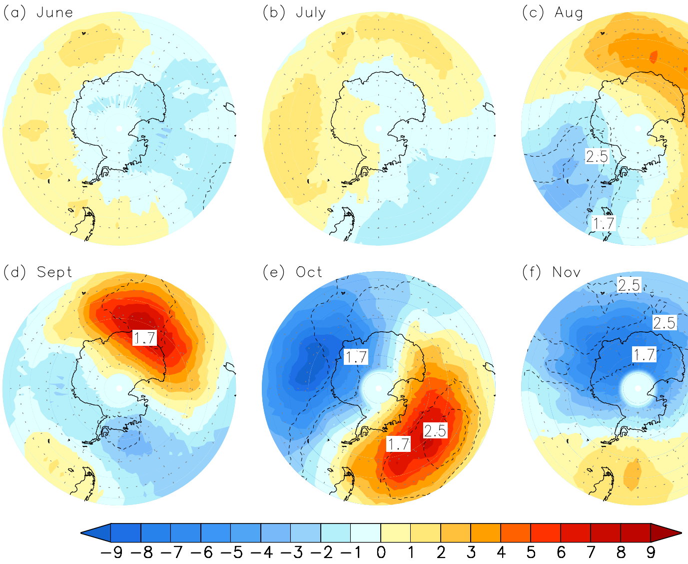

Fig. 1. Temperature trends in the lower stratosphere for 1979–2006 from satellite MSU channel 4 observations. The trends are shown from June to November. Color interval is 1°C per 28 years. Contours denote t-test values. For 28 years, t-test values 1.7 and 2.5 correspond to 90% and 98% confidence levels, respectively.

Title Page
Abstract Introduction
Conclusions References
Tables Figures
◀◀ ▶▶
◀ ▶
Back Close
Full Screen / Esc
Printer-friendly Version
Interactive Discussion

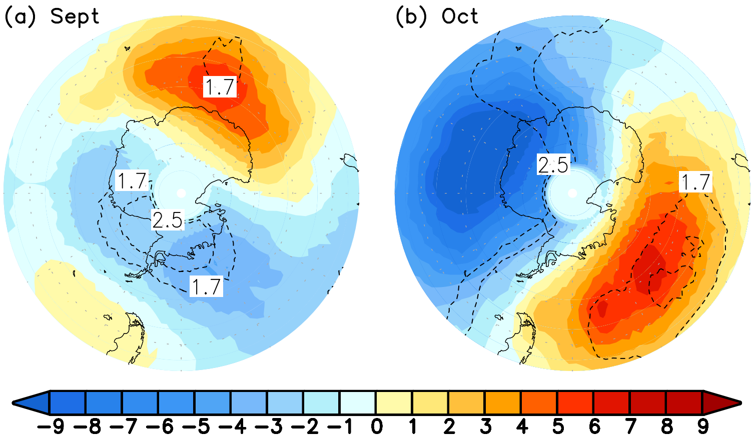

Fig. 2. Same as Fig. 1d and e, except for that year 2002 is excluded.

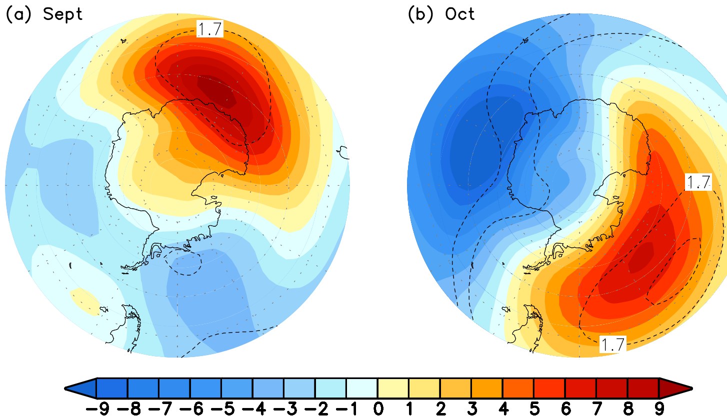

Fig. 3. 28-year (1979–2006) trends in 70 hPa temperatures for September **(a)** and October **(b)**, derived from NCEP/NCAR reanalysis. Color interval is 1° C per 28 years. Contours denote t-test values.

Title Page
Abstract
Introduction
Conclusions
References
Tables
Figures
◀◀
▶▶
◀
▶
Back
Close
Full Screen / Esc
Printer-friendly Version
Interactive Discussion

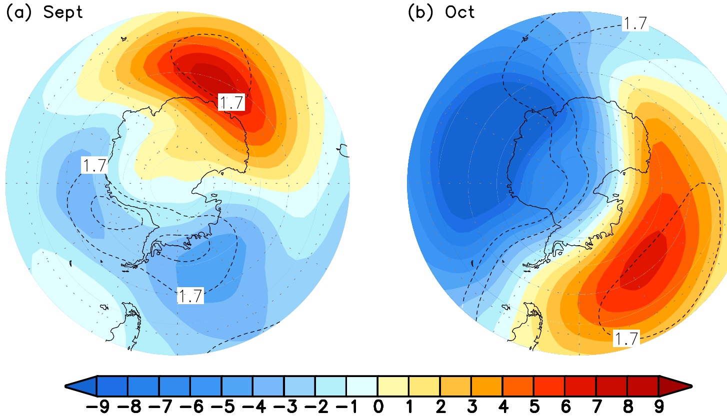

Fig. 4. Same as Fig. 3, except for that year 2002 is excluded.

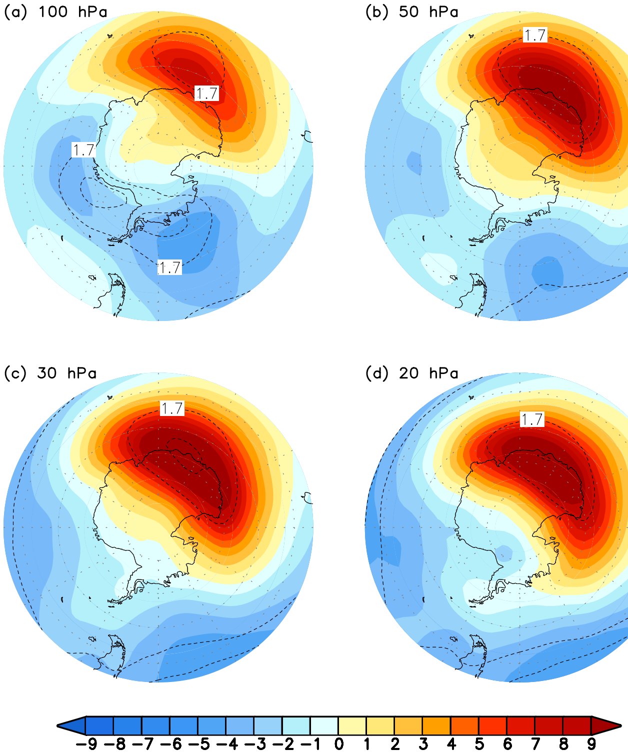

Fig. 5. 28-year temperature trends for September at 100 hPa **(a)**, 50 hPa **(b)**, 30 hPa **(c)**, and 20 hPa **(d)**, derived from NCEP/NCAR reanalysis.

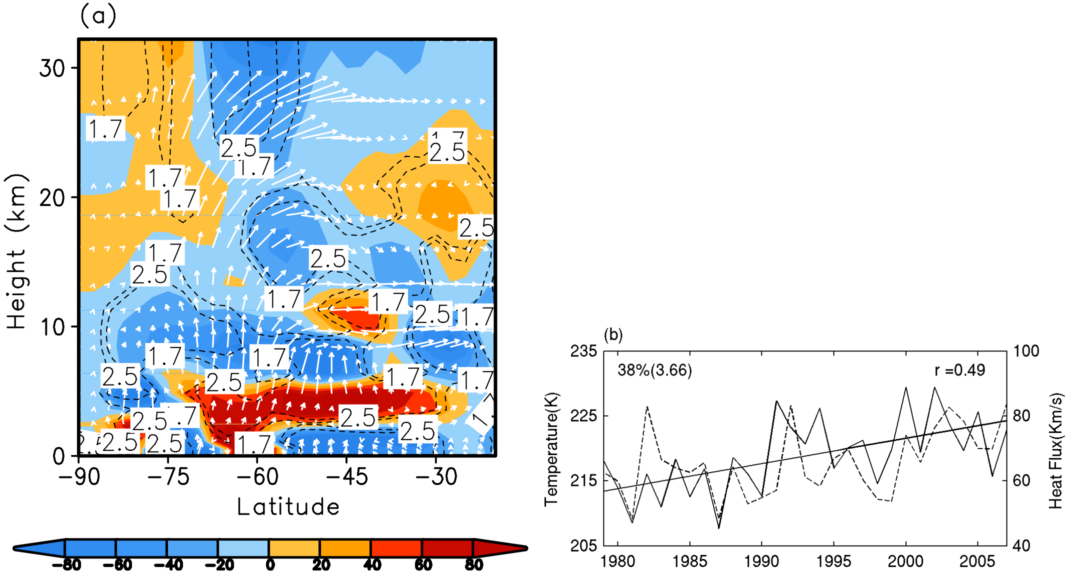

Fig. 6. 28-year trends in EP fluxes **(a)** and eddy-heat fluxes at 150 hPa **(b)** from NCEP/NCAR reanalysis, averaged over August–September–October. In plot **(a)**, arrows, color shading, and dashed contours indicate trends in EP flux vectors, EP flux divergence, and student t-test values. Contours 1.7 and 2.5 indicate statistical significance confidence levels above 90% and 98%, respectively. To show the trends at higher levels, EP flux vectors are divided by the background air density. Because the vertical component of EP fluxes is about two orders smaller than the horizontal component, the vertical component is multiplied by 100 to display changes in wave fluxes in the vertical direction. Trends in EP flux divergence are shown with a color interval of 20 $m^2 s^{-2}$ per 28 years (blue: negative, yellow-red: positive). In plot **(b)**, solid-line is the time series of area-weighted total eddy-heat fluxes at 150 hPa between 90° S and 40° S, and dotted-line is the time series of October temperature at 70 hPa, averaged in the warming area enclosed by the contour of 6°C per 28 years. Values marked in plot **(b)** are the net increase in eddy-heat fluxes in the 28 years (percentage), student t-test (inside bracket), and correlation between temperature and eddy heat fluxes (*r*).

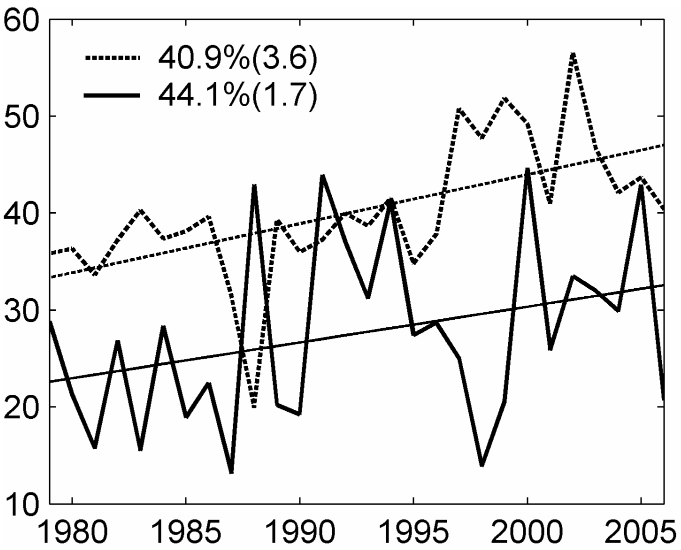

Fig. 7. Same as Fig. 6b, except for heat fluxes due to transient (dashed-line) and stationary (solid line) waves, respectively.

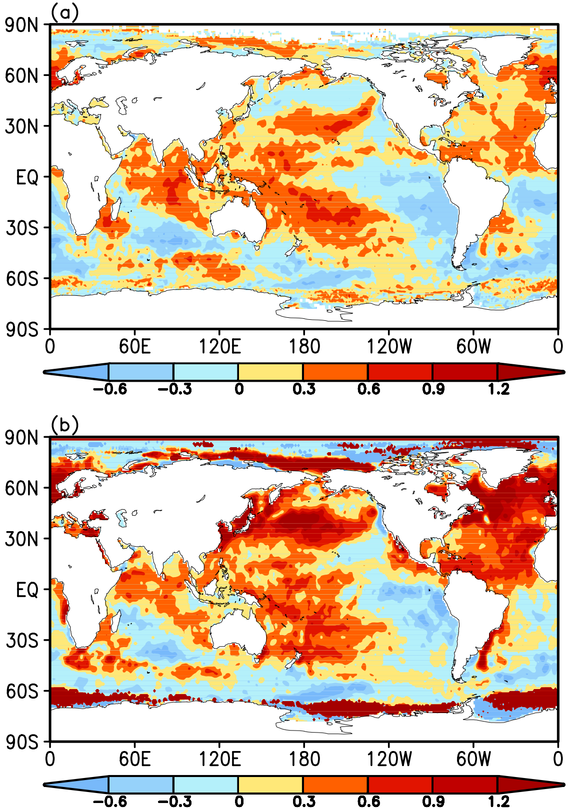

Fig. 8. Relationship between Antarctic stratospheric warming and global SST changes in September. **(a)** Correlation coefficients between a base-point temperature of MSU T_4, averaged over the area enclosed by the contour of 6°C per 28 years, and global observed SST over 1979–2006. Color interval is 0.3. In calculating the correlation coefficients, a 3.5-year filter is used to remove high-frequency variations in both SST and MSU T_4. For 28 years, correlation coefficient of 0.3 approximately marks the 90% confidence level. **(b)** 28-year global SST trends. Color interval is 0.3°C per 28 years.

Title Page
Abstract
Introduction
Conclusions
References
Tables
Figures
◀I
▶I
◀
▶
Back
Close
Full Screen / Esc
Printer-friendly Version
Interactive Discussion

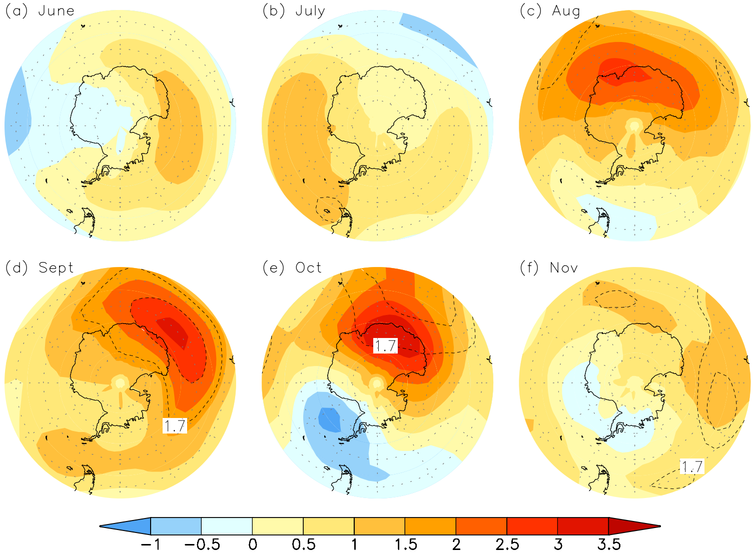

Fig. 9. Temperatures trends at 70 hPa from GCM simulations. The trends are shown from June to November, derived from 5-ensemble simulations. Color interval is 0.5°C per 24 years. Contours denote t-test values.